Smoothed density of states for problems with ray splitting

R. E. Prange, Edward Ott,*,† T. M. Antonsen, Jr.,*,† Bertrand Georgeot, and Reinhold Blümel†

Department of Physics, University of Maryland, College Park, Maryland 20742

(Received 2 August 1995)

Ray splitting is the phenomenon whereby a ray incident on a boundary splits into more than one ray traveling away from the boundary. Motivated by the recent application of ideas of quantum chaos to cases with ray splitting, we present an analysis of the smoothed density of states for two-dimensional billiardlike systems with ray splitting. Using a simple heuristic technique, we obtain a contribution (analogous to the usual perimeter contribution) that is proportional to the length of the ray splitting boundary. The result is expressed in a general form, allowing application to a variety of physical situations. A comparison is also made of the analytical result with numerical data from a particular example.

PACS number(s): 05.45.+b, 03.65.Sq

I. INTRODUCTION

Ray splitting is the phenomenon whereby a ray incident on a sharp boundary splits into more than one ray traveling away from the boundary. For example, a light ray incident on a discontinuity of refractive index splits into a reflected and a transmitted ray. The same thing happens for a plane wave of the Schrödinger equation incident on a discontinuity in the potential $V(\mathbf{r})$ [Fig. 1(a)]. As another example, we note that elastic media support two types of waves, shear (S) and pressure (P) waves, and when an elastic wave is incident on a clamped or free boundary, ray splitting occurs [Fig. 1(b)]. An example where an incident ray splits into four rays at a discontinuity between two elastic media is shown in Fig. 1(c). Other examples of waves that experience ray splitting occur in a variety of physical contexts (e.g., acoustics, microwaves, and plasma waves).

Recently, ideas of quantum chaos have been shown to apply (with suitable modification) to problems with ray splitting [1–3] and attention has focused on billiard-type examples [e.g., Figs. 1(a) and 1(b)]. A basic ingredient in previous quantum chaos studies of billiards is a knowledge of the smoothed level counting function $\bar{N}(E)$. This quantity is a smoothed version of $N(E)$, which gives the number of energy levels with values below E. For the case of a quantum particle of mass m in a simple billiard (without ray splitting) it is found [4–7] that $\bar{N}(E)$ is given by the Weyl formula

$$\bar{N}(E) = \left[\frac{A}{4\pi} \frac{2mE}{\hbar^2} \mp \frac{L}{4\pi} \left[\frac{2mE}{\hbar^2} \right]^{1/2} + K \right] u(E) , \quad (1)$$

where $u(E)$ is the unit step function, A is the area, and L is the perimeter length of the billiard. The quantity K is a number that depends on the topology of the domain

and the curvature and corners of the boundary. For sufficiently large E the contribution from K is small and we shall not consider it further in this paper.

In Eq. (1) the minus sign applies for the case of Dirichlet boundary conditions ($\psi=0$ on the boundary) and the plus sign applies to the case of Neumann boundary conditions ($\partial\psi/\partial n = 0$ on the boundary, where $\partial/\partial n$ denotes the normal derivative). See the work of Balian and Bloch [7] for a full account including the case of the general linear boundary condition $\partial\psi/\partial n = -\kappa\psi$. More general cases were considered in [8].

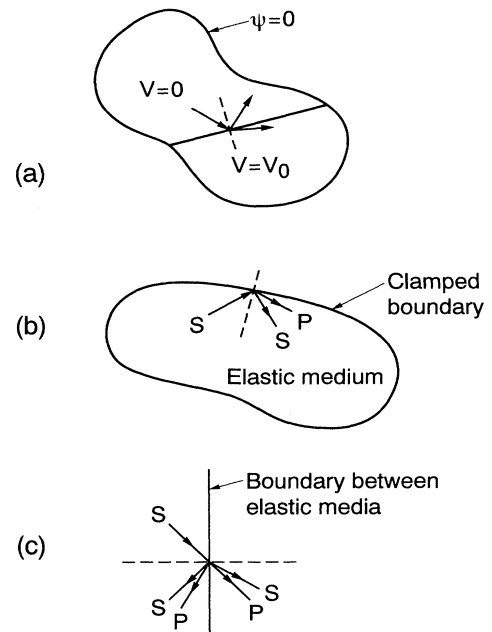The area term is the leading order quasiclassical effect.

FIG. 1. Ray splitting examples. In (b) and (c) the S waves are polarized in the plane of incidence (commonly designated SV waves). For S wave motion polarized perpendicular to the plane of incidence (i.e., SH waves) there is no coupling to P waves at the boundary.

*Also at Department of Electrical Engineering, University of Maryland, College Park, MD 20742.

†Also at Institute for Plasma Research, University of Maryland, College Park, MD 20742.

The correction terms (including that due to ray splitting) are wave corrections arising because the medium changes its properties in a distance short compared to a wavelength at the boundary. The leading corrections can be thought of as a change in effective area by an amount proportional to λL, where λ is the wavelength; e.g., for Dirichlet conditions the area is effectively reduced by an amount $\lambda L / 2\pi$.

Intuitively, it seems natural to suspect that, in cases with ray splitting, there will be a contribution to $\bar{N}(E)$ from the ray splitting boundary and that this contribution will occur at the same order as the perimeter contribution. That is, we suspect that the contribution from a ray splitting boundary will be proportional to $\sqrt{E}$ and to the length of the ray splitting boundary. In this paper we will show that this is indeed the case and we will provide a general expression that yields the ray splitting result in a variety of different physical cases, which we discuss. We will also illustrate our result for the ray splitting contribution by comparison with explicit numerical computations on a particular model example.

II. ANALYSIS

To be specific, first consider the case of the Schrödinger equation in two dimensions with an arbitrary potential $V(\mathbf{r})$, which may have step discontinuities. The eigenstates of this system satisfy $\hat{H}\psi_\alpha = E_\alpha \psi_\alpha$, where

$$\hat{H} = -\frac{\hbar^2}{2m}\nabla^2 + V(\mathbf{r})$$

is the Hamiltonian operator. (Henceforth we take $\hbar = 1$ and $m = \frac{1}{2}$.) The density of states $d(E) = \sum_\alpha \delta(E - E_\alpha)$, where E_α are the energy levels, is formally given by [4–7]

$$d(E) = -\frac{1}{\pi}\mathrm{Im}\{\int d^2\mathbf{r}\, G(\mathbf{r},\mathbf{r},E)\}\ ,\tag{2}$$

where $G(\mathbf{r},\mathbf{r}',E)$ is the Green's function, which satisfies

$$(E - \hat{H})G = \delta(\mathbf{r} - \mathbf{r}')\ ,\tag{3}$$

along with the same boundary conditions that are imposed on the eigenfunctions ψ_α. Equation (2) follows by representing the Green's function as a superposition of the eigenstates

$$G(\mathbf{r},\mathbf{r}',E) = \sum_\alpha \frac{\psi_\alpha(\mathbf{r})\psi_\alpha^*(\mathbf{r}')}{E - E_\alpha + i\epsilon}$$

and noting that $\mathrm{Im}[1/(E - E_\alpha + i\epsilon)] = -\pi\delta(E - E_\alpha)$ when $\epsilon \to 0+$. The level counting function is given by

$$N(E) = \int_{-\infty}^{E} d(E')dE'\ .\tag{4}$$

In order to evaluate the desired contributions to the density of states we can use an approximation to the Green's function. Specifically, the leading term in the smoothed density of states results from replacing the exact Green's function by the free space Green's function. As a result, the shape and location of the boundary do not affect this contribution. To find the perimeter correction, one must do a little better by including contribu-

tions to the Green's function from nearby boundaries. Since these contributions are only important for positions within a wavelength of the boundary, it is adequate to treat the boundary as flat on the scales of interest. With this in mind, we study the problem of all space divided by a ray splitting boundary at $x = 0$. The specific example we consider is that of a potential $V(x,y)$ given by

$$V(x,y) = V_0 u(x)$$

for $-\infty < x$ and $y < +\infty$. Other examples will be treated subsequently. We will then calculate the contribution from the $x = 0$ boundary per unit length in the y direction to $\bar{d}(E)$, the smoothed density of states.

The Green's function for this problem is easily determined by Fourier transforming in the y direction and solving the resulting second-order differential equation in x. For the case in which both the source and observation point are on the left-hand side of the boundary $(x, x' < 0)$ one obtains

$$G(x,x',y,y',E)$$

$$= \int \frac{dk_y}{4\pi i k_x}\exp[ik_y(y - y')]$$

$$\times \{\exp[ik_x|x - x'|]$$

$$+ r(k_y,E)\exp[-ik_x(x + x')]\}\ ,\tag{5}$$

where $r(k_y,E)$ is the reflection coefficient for plane waves incident from the left on the ray splitting boundary. The function $r(k_y,E)$ is determined from the boundary conditions. For the specific case under consideration [i.e., a potential jump $V_0 u(x)$]

$$r(k_y,E) = \frac{k_x - k_x'}{k_x + k_x'}\ ,\tag{6}$$

where k_x and k_x' are the components of the wave vector normal to the surface on the left- and right-hand sides, respectively. These are defined by

$$k_x = \sqrt{E - k_y^2}\tag{7a}$$

and

$$k_x' = \sqrt{E - V_0 - k_y^2}\ .\tag{7b}$$

Since the transform variable k_y extends from $-\infty$ to $+\infty$, one must specify the way in which the square root in Eqs. (7) is to be taken. The conditions on the Green's function at $|x| \to +\infty$ require that k_x and k_x' be positive if they are real and positive imaginary otherwise. This allows the Fourier inversion in (5) to be viewed as a contour integral in the complex k_y plane, which is deformed around the branch points at $k_y = \pm\sqrt{E}$ and $k_y = \pm\sqrt{E - V_0}$, as shown in Fig. 2. We now evaluate the contributions to Eq. (2) from the left half space by setting $x = x'$ and $y = y'$ and integrating over x and y.

The first term in the Green's function (5) is the free space contribution and gives, as mentioned, the lowest-order density of states when integrated over the relevant area in the full problem. The second term gives the effect
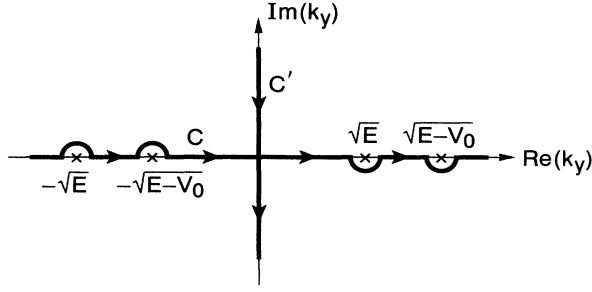
FIG. 2. Contours C and C' in the complex k_y plane.

of the boundary and will be proportional to the length of the ray splitting boundary L_{RS}. We thus obtain for the boundary contribution, after integrating over x from $-\infty$ to 0,

$$\bar{d}_B(E) = \frac{L_{RS}}{8\pi^2} \text{Im} \left\{ \int_C \frac{dk_y}{k_y^2 - E} r(k_y, E) \right\}, \qquad (8)$$

where C labels the contour depicted in Fig. 2. (In three dimensions x,y,z the term in curly brackets in (8) is replaced by $\int_C r(k_\perp, E)[k_\perp^2 - E]^{-1} k_\perp dk_\perp$, where now C runs from $k_\perp = 0$ to ∞, circling below the points $k_\perp = \sqrt{E}, \sqrt{E - V_0}$.)

It is important to note that Eq. (8) is actually more general than the derivation first indicates because we have yet to use any specific information on the particular form of the reflection coefficient. Thus (8) applies for the Helmholz equation with any appropriate set of boundary conditions. To illustrate this, we note that if the ray splitting boundary is replaced by one with Neumann or Dirichlet conditions on the wave function, the appropriate reflection coefficient is $r = +1$ or -1, respectively. In this case the integral in Eq. (8) can be evaluated by closing the contour in the upper half plane and picking up the residue from the pole at $k_y = \sqrt{E}$. One obtains

$$\bar{d}_B(E) = \frac{L_{RS} r}{8\pi E^{1/2}}. \qquad (9)$$

Integrating over energy to obtain $\bar{N}(E)$ gives precisely the perimeter correction of Eq. (1).

As another check on Eq. (8) we may also apply it to the case of a mixed boundary condition $\partial\psi/\partial n = -\kappa\psi$. In this case the reflection coefficient is $r(k_y, E) = (ik_x - \kappa)/(ik_x + \kappa)$. The integral Eq. (8) may then be evaluated by deforming the contour to C' as shown in Fig. 2 and setting $k_y = -i\sigma$. The boundary contribution to the density of states is then given by

$$\bar{d}_B(E) = \frac{L_{RS}}{8\pi^2} \int_{-\infty}^{\infty} \frac{d\sigma}{E + \sigma^2} \frac{E + \sigma^2 - \kappa^2}{E + \sigma^2 + \kappa^2}.$$

Evaluating the integral, we obtain a result in agreement with Balian and Bloch [7,9],

$$\bar{d}_B(E) = \frac{L_{RS}}{8\pi} \left[-\frac{1}{E^{1/2}} + \frac{2}{(E + \kappa^2)^{1/2}} \right]. \qquad (10)$$

Thus, as one might expect, at low energies the boundary term behaves as in the Dirichlet case and at high energy $(E \gg \kappa^2)$ the behavior is as in the Neumann case.

We now return to the problem of the ray splitting step discontinuity and evaluate its contribution to the smoothed density of states. Equation (8) gives only the contribution from the left-hand side of the ray splitting boundary. By inspection we can add in the contributions from the right-hand side

$$\bar{d}_B(E) = \frac{L_{RS}}{8\pi^2} \text{Im} \left\{ \int_C dk_y \left[\frac{r(k_y, E)}{k_y^2 - E} + \frac{r'(k_y, E)}{k_y^2 + V_0 - E} \right] \right\}, \qquad (11)$$

where $r'(k_y, E) = -r(k_y, E)$ is the reflection coefficient for plane waves incident from the right. If one carries out the integration along the contour C in Fig. 2, there are two types of contribution to the imaginary part of the integral in Eq. (11). The first is contributions from the semicircular arcs around the points $k_y = \pm\sqrt{E}$ and $k_y = \pm\sqrt{E - V_0}$ (if $E > V_0$). This contribution may be written

$$\bar{d}_{B1} = -\frac{L_{RS}}{8\pi} \left[\frac{u(E)}{E^{1/2}} + \frac{u(E - V_0)}{(E - V_0)^{1/2}} \right], \qquad (12)$$

where $u(E)$ is the unit step function. The second contribution comes from the portion of the contour along which the reflection coefficient has an imaginary part. For $0 < E < V_0$ this corresponds to $|k_y| < \sqrt{E}$ and for $V_0 < E$ this corresponds to $\sqrt{E - V_0} < |k_y| < \sqrt{E}$. Writing $k_y = \sqrt{E} \sin\alpha$, where α is the angle of incidence of a plane wave on the left-hand side, we see that the contributions come from angles for which there is total internal reflection. Specifically, for $E > V_0$ the contributions come from angles satisfying $\alpha_c < \alpha < \pi/2$, where $\alpha_c = \sin^{-1}(\sqrt{1 - V_0/E})$ is the critical angle for total internal reflection. Using the expression (6) for the reflection coefficient, this contribution can be written

$$\bar{d}_{B2} = \frac{L_{RS}}{2\pi^2} \int_{k_m}^{E^{1/2}} \frac{dk_y}{\sqrt{E - k_y^2}\sqrt{V_0 - E + k_y^2}}, \qquad (13)$$

where $k_m = 0$ if $E < V_0$ and $k_m = \sqrt{E - V_0}$ if $E > V_0$. Introducing the variable $z = E/V_0$, the contribution (13) may be expressed in terms of $K(k) = \int_0^{\pi/2} d\theta (1 - k^2 \sin^2\theta)^{-1/2}$, the complete elliptic integral of the first kind

$$\bar{d}_{B2} = \frac{L_{RS}}{2\pi^2} \frac{K(z^{-1/2})}{V_0^{1/2}}$$

for $z < 1$ and

$$\bar{d}_{B2} = \frac{L_{RS}}{2\pi^2} \frac{K(z^{1/2})}{(zV_0)^{1/2}}$$

for $z > 1$. Combining the two contributions and integrating over energy gives the contribution $\Delta\bar{N}(E)$ from ray splitting to the level counting function

$$\frac{\Delta \bar{N}(E)}{L_{rs}} = -\sqrt{V_0}\left[\frac{\sqrt{z}}{4\pi}u(z) - \frac{u(z)-u(z-1)}{2\pi^2}\right.$$

$$\left. \times \int_0^z K(\sqrt{\bar{z}})d\bar{z}\right] - \sqrt{V_0}\left[\frac{\sqrt{z-1}}{4\pi}-\frac{1}{\pi^2}\right.$$

$$\left. -\frac{1}{2\pi^2}\int_1^z \frac{K(\bar{z}^{-1/2})}{\sqrt{\bar{z}}}d\bar{z}\right]u(z-1). \qquad (14)$$

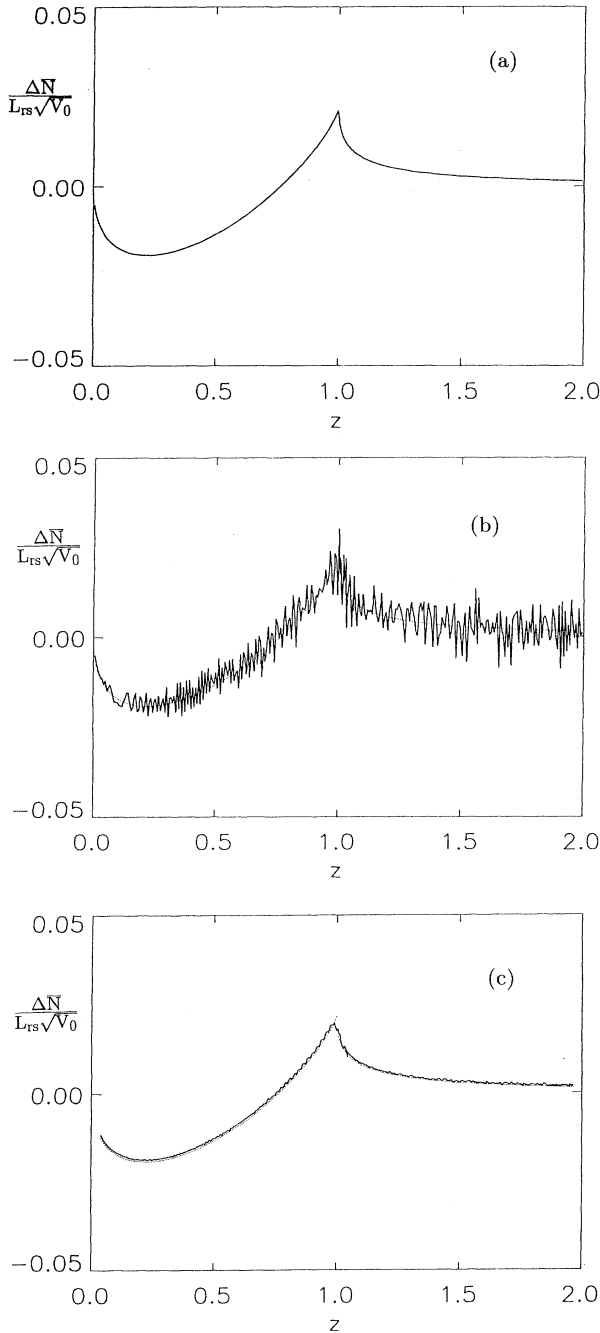In Fig. 3(a) we plot $\Delta \bar{N}(E)/L_{\rm RS}\sqrt{V_0}$ as a function of z.

Note the discontinuity at $z=1$. Also note that $\Delta \bar{N}$ from (14) is generally smaller in magnitude than the Dirichlet and Neumann values $\Delta \bar{N}/L = \mp \sqrt{E}/4\pi$. The integrals in Eq. (14) can be evaluated in terms of complete elliptic integrals if desired.

As a numerical check on Eq. (14) we consider the model problem shown in Fig. 4, where the boundary condition on the side walls is taken to be Dirichlet and on the upper and lower walls is taken to be Neumann. Continuity of the wave function and its normal at the ray splitting boundary give the energy levels as the solutions of a transcendental equation

$$[E-(n\pi/L_0)^2]^{-1/2}\tan\{[E-(n\pi/L_0)^2]^{1/2}L_1\}$$

$$+[E-V_0-(n\pi/L_0)^2]^{-1/2}$$

$$\times \tan\{[E-V_0-(n\pi/L_0)^2]^{1/2}L_2\}=0 , \qquad (15)$$

where for Neumann boundary conditions (cf. Fig. 4) on the top and bottom walls we have $n=0,1,2,\ldots$. Taking $V_0=10^5$ and $L_1=L_2=L_0/2$, we have numerically solved for the energy levels from $E=0$ to 2×10^5. (The second term in (15) becomes $[(n\pi/L_0)^2-E+V_0]^{1/2}\tanh\{[(n\pi/L)^2-E+V_0]^{1/2}L_2\}$ when $E<V_0+(n\pi/L_0)^2$.) Using these we obtain the level counting function $N(E)$. Using (1) to subtract out the area contribution, we obtain the residual $\Delta N(E)$. The quantity $\Delta N(E)$ shows rapid fluctuations with energy, as one expects (there are continuous families of classical periodic orbits). Smoothing $\Delta N(E)$ over 50 levels, we obtain the numerical $\Delta \bar{N}(E)$ shown in Fig. 3(b). Smoothing over $\sim 10^3$ levels we obtain Fig. 3(c). The dotted lines in Figs. 3(b) and 3(c) are the theory. Because we take Dirichlet boundary conditions on the side walls and Neumann boundary conditions on the top and bottom walls, the contribution to the perimeter term from the walls is precisely zero $(L_1=L_2=L_0/2)$. Thus, at lowest order, $\Delta \bar{N}(E)$ is due solely to the ray splitting boundary. The agreement between the results from the numerical solution of (15) and the theoretical curve is very good.
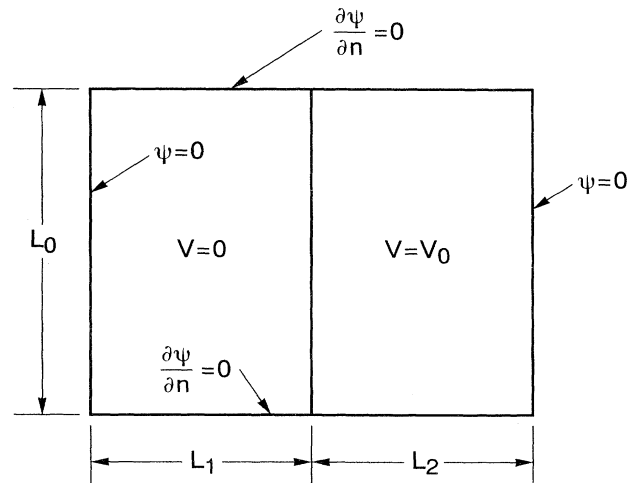

FIG. 3. $\Delta \bar{N}/(L_{\rm RS}\sqrt{V_0})$ versus z.

FIG. 4. Model problem.

III. OTHER APPLICATIONS

So far we have restricted the discussion to the case of the Schrödinger equation with a discontinuity in potential. The analysis, however, is readily applied to other physical situations. Several of these are discussed below.

Case 1: Schrödinger equation with a δ-function potential. Using $V(\mathbf{r}) = v_0 \delta(x)$ in place of $V(\mathbf{r}) = V_0 u(x)$, we have a ray splitting boundary of a somewhat different type than that considered above. In particular, although an incident wave is still reflected and transmitted, there is no refraction of the propagation direction upon transmission and hence no total internal reflection. An elementary calculation yields the reflection coefficient

$$r(E) = -[1 - 2ik_x/v_0]^{-1} \qquad (16)$$

and $r'(E) = r(E)$ by the symmetry of the potential. Thus $\Delta \overline{N}(E)$ is given by (8) [with (16) used for r] multiplied by a factor of 2 to account for the two sides of the ray splitting boundary.

The integral may be evaluated by switching to the contour C' in Fig. 2 with the result

$$\overline{d}_B(E) = \frac{L_{RS}}{4\pi} \left[\frac{1}{\sqrt{E + (v_0/2)^2}} - \frac{1}{\sqrt{E}} \right] , \qquad (17)$$

which has a somewhat analogous character to that for the mixed boundary condition Eq. (10).

Case 2: Thin microwave cavity with a discontinuity in height. Now consider a vacuum filled microwave cavity that is very thin in the z direction. The quantity of interest here is $N(\omega)$, the number of cavity resonant modes with frequencies below ω. Since the cavity is thin in the z direction, the z component of the electric field satisfies the two-dimensional Helmholtz equation in x and y,

$$(\nabla_{x,y}^2 + k^2)E_z = 0 ,$$

where $k^2 = \omega^2/c^2$, c is the speed of light, and E_z satisfies a Dirichlet boundary condition on the bounding curve. This situation has received much attention as a convenient experimental system for studying quantum chaos [10]. In Ref. [2] it was suggested that ray splitting could be introduced in such a system by introducing a discontinuity in the vertical height of the cavity. Say the height is h in $x < 0$ and h' in $x > 0$. For wavelengths large compared to h and h', the boundary conditions on the electric field E_z are continuity of $\partial E_z/\partial y$ and continuity the voltage between the upper and lower plates [i.e., $hE_z(x = 0-) = h'E_z(x = 0+)$]. One obtains reflection coefficients r and r' that are real and independent of energy and angle [2],

$$r = -r' = (h' - h)/(h' + h) . \qquad (18)$$

As a consequence of $r = -r'$, Eq. (8) yields precisely zero for $d_B(\omega)$ when the contribution from the two sides are added. This is easily understood in the case $h'/h \to 0$. In this case the two sides decouple into two independent cavities, one with a Dirichlet boundary condition ($r = -1$) and one with a Neumann boundary condition ($r = +1$). When the two $\overline{N}(\omega)$ for each side are added

the Dirichlet decrease on one side ($x < 0$) is precisely canceled by the Neumann increase on the other side ($x > 0$).

Case 3: Scaled Schrödinger problem. We now consider a "scaled" Schrödinger problem defined by replacing V_0 in $\{\nabla^2 + [E - V_0 u(x)]\}\psi = 0$ by $V_0 = \eta E$ (i.e., we vary V_0 with E) to obtain

$$\{\nabla^2 + [1 - \eta u(x)]E\}\psi = 0 . \qquad (19)$$

[Here $\eta > 0$ and $u(x)$ can be the step or, more generally, any non-negative function.] For this scaled problem we ask what is the number of eigenvalues $N_s(E, \eta)$ below E when η is held fixed. As shown schematically in Fig. 5, the level counting function $N_s(E_*, \eta)$ for the scaled problem at energy $E = E_*$ and scaling parameter η is the number of net crossings from left to right of the dash-dotted line $E/V_0 = \eta \equiv E_*/V_*$ by E_α versus V_0 curves. The level counting function $N_{us}(E_*, V_*)$ for the unscaled problem at constant potential V_* and at energy E_* is the number of crossings of the vertical dashed line by E_α versus V_0 curves. We claim that this number is the same: $N_s(E_*, \eta)$ at $\eta = E_*/V_*$ is equal to $N_{us}(E_*, V_*)$ at $V_0 = V_*$. To prove this, we need the positivity of E_α ($V_0 > 0$) and we need to show that

$$dE_\alpha/dV_0 < E_\alpha/V_0 ; \qquad (20)$$

i.e., once an E_α versus V_0 curve crosses the line $E/V_0 = \eta$, it never crosses back. An energy level of the unscaled problem is given by

$$E_\alpha = (\psi_\alpha, H\psi_\alpha) , \qquad (21)$$

where $H = -\nabla^2 + V_0 u(x)$. Differentiating (21) with respect to V_0, we have

$$dE_\alpha/dV_0 = (\psi_\alpha, u(x)\psi_\alpha) , \qquad (22)$$

where derivatives of ψ_α with respect to V_0 do not contribute due to the variational property of H. Using (21) to reexpress the right-hand side of (22) as $(E_\alpha/V_0) + (\psi_\alpha, \nabla^2 \psi_\alpha)$ and noting the negativity of $(\psi_\alpha, \nabla^2 \psi_\alpha)$, we obtain (20), which proves our assertion that $N_s(E, \eta) = N_{us}(E, V_0)$ when $V_0 = \eta E$. Note, however, that the corresponding densities of states $d_{us}(E, V_0) = (\partial N_{us}/\partial E)_{V_0}$ and $d_s(E, \eta) = (\partial N_s/\partial E)_\eta$ are
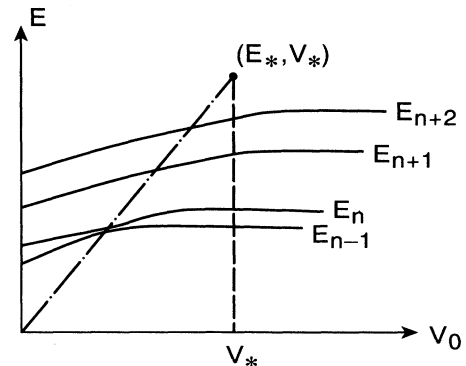
FIG. 5. Schematic illustration of E_α versus V_0.

unequal. For example,

$$d_s(E,\eta)=d_{us}(E,V_0)+\eta^{-1}(\partial N_{us}/\partial V_0)_E \ .$$

Case 4: Thin microwave cavity with a discontinuity in dielectric constant. Again consider a thin microwave cavity, but this time one with a constant height. Assume that there is a dielectric of relative dielectric constant ϵ in $x<0$ and a dielectric of relative dielectric constant ϵ' in $x>0$. Then the phase velocity of plane waves is $v=c/\sqrt{\epsilon}$ in $x<0$ and $v'=c/\sqrt{\epsilon'}$ in $x>0$. For $\epsilon>\epsilon'$ there can be total internal reflection for waves incident on the $x=0$ boundary from $x<0$. This problem for $N(\omega)$ is formally the same as the scaled Schrödinger problem with a step potential as can be seen by writing the wave equation for E_z as

$$\left[\nabla^2+\frac{\omega^2}{v^2}\{1-[1-(v/v')^2]u(x)\}\right]E_z=0 \ . \tag{23}$$

Equation (14) can then be used to obtain $\Delta\bar{N}(\omega)$ by replacing E by $(\omega/v)^2$ and V_0 by $(\omega/v)^2[1-(v/v')^2]$.

Case 5: Elastic medium billiard with a clamped or free boundary. This case [Fig. 1(b)] is considered in the context of quantum chaos in Ref. [1]. Let v denote the velocity of S waves and v' the velocity of P waves. The displacement $\mathbf{u}$ of a point in the elastic medium due to waves may be expressed in terms of a scalar and a vector potential $\mathbf{u}=\nabla\phi'+\nabla\times\mathbf{A}$, which give the P and S wave components, respectively. Setting $\mathbf{A}=\mathbf{z}_0\phi$ [appropriate to two dimensions and vertical polarization of the S wave; Fig. 1(b)], the S wave potential ϕ and the P wave potential ϕ' both satisfy Helmholtz equations

$$(\nabla^2+k^2)\phi=0$$

and

$$[\nabla^2+(k')^2]\phi'=0 \ ,$$

where $k=\omega/v$ and $k'=\omega/v'$. The S and P wave fields are coupled through boundary conditions at the billiard edge. Thus we are again dealing with a scaled problem very similar to that of the microwave cavity containing a discontinuity in dielectric constant.

As before, the boundary conditions require the satisfaction of Snell's law for this problem, $(\omega/v)\sin\alpha=(\omega/v')\sin\alpha'$, where α (α') is the S wave (P wave) propagation angle to the normal to the boundary. Since the shear wave velocity is slower than the pressure wave velocity $v<v'$, Snell's law implies that there is an angle for total internal reflection of S waves (but not P waves). Thus the S waves are analogous to the waves in the $x<0$ region of the Schrödinger problem with the step potential and the P waves are analogous to the waves in the $x>0$ region of the Schrödinger problem. Using this analogy we can apply Eq. (11) as follows. Let r (r') denote the reflection coefficient for conversion of an incident S wave (P wave) to a reflected S wave (P wave). [Note that the expressions for r and r' in this case are *different* from (6) so that (14) does not apply.] In the expressions for r and r' now make the replacements $(\omega/v)\rightarrow\sqrt{E}$ and $(\omega/v')\rightarrow\sqrt{E-V_0}$. Then put the result into (11) and do the integration with respect to E. After this is done convert back via $E\rightarrow(\omega/v)^2$ and $V_0\rightarrow(\omega/v)^2[1-(v/v')^2]$ to obtain $\Delta\bar{N}(\omega)$,

$$\Delta\bar{N}(\omega)=\frac{L_{RS}}{8\pi^2}\int_0^{(\omega/v)^2}\text{Im}\left\{\int_C dk_y\left[\frac{r(k_y,\bar{E})}{k_y^2-\bar{E}}+\frac{r'(k_y,\bar{E})}{k_y^2+\frac{\omega^2\delta}{v^2}-\bar{E}}\right]\right\}d\bar{E} \ , \tag{24}$$

where $\delta=[1-(v/v')^2]$.

As a specific example consider the case of a clamped boundary ($\mathbf{u}\equiv0$ on the boundary). Using $\mathbf{u}=\nabla\phi'-\mathbf{z}_0\times\nabla\phi$, we obtain the reflection coefficients

$$r=r'=\frac{k_xk_x'-k_y^2}{k_xk_x'+k_y^2} \ , \tag{25}$$

where $k_x=(k^2-k_y^2)^{1/2}$ and $k_x'=[(k')^2-k_y^2]^{1/2}$. [In the case of a free boundary the boundary condition is $\mathbf{n}\cdot\mathbf{T}=0$, where $\mathbf{n}$ is the unit normal and $\mathbf{T}$ is the stress tensor (see, e.g., Ref. [1] for r in this case).] To obtain $\Delta\bar{N}(\omega)$ for this problem we thus write

$$k_x=\sqrt{E-k_y^2} \ , \quad k_x'=\sqrt{E(1-\delta)-k_y^2} \ , \tag{26}$$

substitute (26) in (25), and put the result in (24). This yields

$$\Delta\bar{N}(\omega)=(8\pi)^{-1}(\omega L_{RS}/v)F(\delta) \ , \tag{27a}$$

$$F(\delta)\equiv\int_0^1 dz\ \text{Im}\left[\int_C d\eta\frac{\sqrt{z-\eta^2}\sqrt{z-\delta-\eta^2}-\eta^2}{\sqrt{z-\eta^2}\sqrt{z-\delta-\eta^2}+\eta^2}\right.$$
$$\left.\times\left[\frac{1}{\eta^2-z}+\frac{1}{\eta^2+\delta-z}\right]\right] \ . \tag{27b}$$

Thus the same result [Eq. (11)] yields the leading-order ray splitting contribution to the smoothed level counting function in a variety of physical situations [11,12].

ACKNOWLEDGMENTS

[1] L. Couchman, E. Ott, and T. M. Antonsen, Jr., Phys. Rev. A **46**, 6193 (1992).

[2] R. N. Oerter, E. Ott, T. M. Antonsen, Jr., and P. So (unpublished).

[3] R. Blümel, T. M. Antonsen, Jr., B. Georgeot, E. Ott, and R. E. Prange (unpublished).

[4] A. M. Ozorio de Almeida, *Hamiltonian Systems: Chaos and Quantization* (Cambridge University Press, Cambridge, 1988).

[5] M. C. Gutzwiller, *Chaos in Classical and Quantum Mechanics* (Springer-Verlag, Berlin, 1990).

[6] E. Ott, *Chaos in Dyanmical Systems* (Cambridge University Press, Cambridge, 1993), Chap. 10.

[7] R. B. Balian and C. Bloch, Ann. Phys. (N.Y.) **60**, 401 (1970); **63**, 592 (1971); **64**, 271 (1971).

[8] D. J. Vasil'ev, Trans. Moscow Math. Soc. **49**, 173 (1987). This paper's result also includes the possibility of ray splitting although the situation studied does not apply to any of the cases we consider [e.g., Fig. 1(a)].

[9] See also M. Sieber, H. Primack, U. Smilansky, I. Ussishkin, and H. Schanz (unpublished).

[10] For example, H.-J. Stockmann and J. Stein, Phys. Rev. Lett. **64**, 2215 (1990); S. Sridhar, *ibid.* **67**, 785 (1991); H. D. Graf *et al.*, *ibid.* **69**, 1296 (1992); P. So, S. M. Anlage, E. Ott, and R. N. Oerter, *ibid.* **74**, 2662 (1995).

[11] The situation in Fig. 1(c) can also be treated by summing four contributions of the form of (8) corresponding to the four reflection coefficients, one for S waves incident from $x < 0$ converted to reflected S waves in $x < 0$ and similar reflection coefficients for P waves incident from $x < 0$, S waves incident from $x > 0$, and P waves incident from $x > 0$.

[12] Quantum chaos experiments in elastic media have recently been done [R. L. Weaver, J. Acoust. Soc. Am. **85**, 1001 (1989); D. Delande, D. Sornette, and R. Weaver, J. Acoust. Soc. Am. **93**, 1873 (1994); C. Ellegard *et al.*, Phys. Rev. Lett. **75**, 1546 (1996)].